Automatic Detection and Counting of Small Airborne Dust Particles

Sylvia Leimgruber, Frank Lenzen and Otmar Scherzer
Department of Computer Science, LFU Innsbruck.

sylvia.leimgruber@uibk.ac.at

Abstract:
In the Institute of Botany at the University of Innsbruck pollen samples have been collected continuously 24 hours a day since 1977. With hindsight the statistical evaluation of the complete set of samples would allow important insights into the air quality in the Innsbruck region over the past 30 years. This region is exposed to increased air pollution due to the high traffic concentration on the Inn valley and Brenner motor-ways. The aim of this project is an automated analysis of the samples with respect to airborne particles using digital imaging methods to analyze and recognize number and size of the particles. Scanning the sample surface, saving the digital image data, analyzing the airborne particles and statistical processing of the collected aerobiological data is intended to be a fully automated process. The complete instrument control and analysis should be implemented within a single software environment on a personal computer.

1 Introduction

Small airborne dust particles, known as particulate matter (PM), are a serious health concern when inhaled since they can penetrate deeply into the respiratory tract where they accumulate. In medical research, particular attention has been devoted to particles less than 10 micrometers in diameter (PM_{10}) which are supposed to be responsible to aggravated cardiac and respiratory (heart and lung) diseases in addition to increased cancer risk and premature death. These small particles are a product of combustion processes, especially of diesel fuel. They are due to air pollutant emission by a number of sources from industrial power plants and motor-vehicles. Other sources comprise windblown dust, brake lining and tire wear ([3],[9]). To analyze the evolution of air pollutant caused by PM_{10}, aerobiological data preserved by the Institut of Botany in Innsbruck over many years are available.

In section 2 a methodological background of the preparation technique used for pollen samples is given. In section 3 the current algorithm for recognizing of the particles is explained, including pre- and postprocessing steps. Section 4 presents results of a numerical classification.

And in section 5 we discuss the applicability of a beta-version of our algorithm for particle detection.

2 Background

The Institute of Botany at the University of Innsbruck, led by Prof. Dr. Bortenschlager, in a joint project with the Pollen Information Service Tyrol provides data on the present airborne pollen dispersion and analyzes the pollen flight for regions at different altitudes in Tyrol ([1]). These informations should help people suffering from pollen allergy to avoid the contact with those particles as far as possible. The record of pollen emission measurements started 1977 with three pollen traps located in the valley areas of Innsbruck, Wörgl and Imst. 1980 three additional pollen traps were installed in Obergurgl, Kühtai and Galtür. At the present in Tyrol 11 pollen traps are installed. The pollen records are performed using the Burkard pollen trap ([11]), which absorbs 10 liters of air per minute, corresponding approximately to the human inhalation, through a narrow orifice of 2mm×14mm. The airborne particles are collected on an adhesive plastic tape, mounted on a clockwork-driven drum, which rotates once a week at the speed of 2 mm per hour. The exposed part of the tape is removed from the drum and is cut into daily periods, corresponding to 48 mm segments with a sampling rate of 1 hour time resolution. After embedding the tape onto standard microscope slides with a Gelvatol solution, the daily samples are analyzed in a conventional light microscope. The archived areobiological samples of the Institut of Botany over many years and the high trap collection efficiency, particularly for particles less than 10 μm in diameter, makes the effort to reanalyze the sample sets with respect to PM_{10} more than self-evident.

3 Strategy and Algorithm

The beta-version of our detection algorithm developed for identifying and counting airborne dust particles less than 10 μm in diameter consists mainly in the following subsystems:

1. Microscopic scanning of the biological samples to obtain digital images.
2. Preprocessing of the digital images, which includes extension of depth-of-field, consistency checks and image filtering.
3. Image segmentation and postprocessing with morphological filtering techniques.
4. Classification of the segmented objects, in particular PM_{10}.

The algorithm described in detail below has been implemented in the programming language C. The digital image processing is done on a Intel®Pentium®4 with 1.5 GHz CPU, 1024 MByte RAM and Unix operating system. The microscopy imaging is performed with a Olympus VANTOX/T microscope with an on-board Sony CCD-camera. Initially stacks of

microscope greyscale images at a resolution of 760×570 pixels are acquired at different focal planes. The images have to be aligned throughout the stack and must be at the same microscope magnification.

Throughout the paper the following notation is used: The images are considered as two-dimensional intensity arrays $\{(x, y); 1 \leq x \leq m, 1 \leq y \leq n\}$ with greyscale pixel data; $s(x, y; z_k)$ represents the kth slice of the image stack $\{s(x, y; z_k)\}_z$ in z-direction; for a pixel at position (x, y) the index into the image array is given as a non-negative value in the range of 0 to $mn - 1$.

3.1 Preprocessing Steps

3.1.1 Image Fusion Algorithm

In microscopy imaging with an conventional light microscope one has normally to deal with the problem of limited depth-of-field. Only a small area of each microscopic section of a sample will be in focus, most of the areas appear defocused. One common approach to extend the depth-of-field is by taking multiple images by moving the focal plane serially through the sample and selecting from each slice the areas where sharp features are present. In that way it is possible to achieve an image projection of the sample that is in focus everywhere, which is more suitable for image processing tasks such as segmentation and object recognition. Methods for extending the depth-of-field in an image have been proposed by a number authors, an overview can be found in [7]. There are three different approaches for image fusion algorithms, on point process basis, on an neighborhood process basis and on the multi resolution process basis respectively. The basic approach of all algorithms is, that initially an image stack $\{s(x, y; z_k)\}_k$ is generated, where k is the number of images taken. Then for all image slices $s(x, y; z_k)$ every pixel is scanned and for every pixel position (x, y) an in-focus measure is computed for each respective slice. The pixel with the best measure is selected, according to sharpness criteria regarding the different fusion algorithms and is built up to a composite image $s(x, y)$. Since a useful feature in an image usually is larger than one pixel, the point-based image fusion may not be an appropriate method, therefore we used the area-based variance method. The variance method is based on the assumption that larger variations of intensity occur in the regions of the image that are in focus. The variance $\sigma(x, y; z_k)$ for each pixel position (x, y) of $s(x, y; z_k)$ over a 3×3 pixels neighborhood is computed. In our implementation we used the maximum absolute-value selection rule, since the largest absolute value indicates the presence of a salient feature in the local area. At each position (x, y) the pixel along the z-axis with the highest variance is chosen for the composite image.
As a multiresolution-based fusion algorithm we tested the complex wavelet method by using the freely available software provided by [2], which applies the complex wavelet transform for multi resolution image fusion in the wavelet domain. This method seems to be more sensitive

to translucent objects compared to the variance method.

3.1.2 Consistency Checks

A topological map $M(x, y)$, $1 \leq x \leq m$ and $1 \leq y \leq n$, is created by recording the numbers of the selected slices based on the maximum absolute-value selection rule σ:

$$M(x, y) := \arg\max_k |\sigma(s(x, y; z_k))|.$$

This map is subject to consistency checks. There are several approaches on consistency checks. We applied the majority filter as a spatial consistency check to the topological map M, i.e. if the center map value in a 3×3 map patch comes from slice l while the majority of the surrounding entries are from a different slice $k \neq l$, then the value of the $M(x, y) = l$ is changed to $M(x, y) = k$. Finally a composite image is obtained based on the topological map M:

$$s(x, y) = s(x, y; M(x, y)) \quad \forall\ (x, y).$$

3.1.3 Image Filtering

We smooth the recorded images by the anisotropic diffusion ([4],[8]), which has the advantage of reducing noise while preserving contours in the images.
Anisotropic diffusion filtering consists in solving the time dependent differential equation

$$\partial_t u(t, x, y) - \nabla \cdot (D(\nabla u)\nabla u(t, x, y)) = 0,$$

using the given data $s(x, y)$ defined on domain $\Omega \subset \mathbb{R}^2$ as initial condition at the time $t = 0$,

$$u(0, x, y) = s(x, y) \text{ on } \Omega,$$

and homogeneous Neumann boundary conditions

$$\frac{\partial u}{\partial n}(t, x, y) = 0 \ \text{ on } (0, T) \times \partial\Omega$$

up to a certain time T. The diffusion tensor $D(\nabla u_\sigma)$ is locally adapted to a presmoothed version u_σ of the image, to provide linear diffusion in homogeneous regions and diffusion parallel to edges in regions with high intensity gradients. The filtered image given by $u(T, x, y)$ then is used as input in the subsequent segmentation step described in section 3.2.1.

3.2 Image Segmentation and Object Classification

3.2.1 Object Finding

Image segmentation is an essential component in any image analysis and pattern recognition and is one of the most difficult tasks, since it determines the quantitative interpretation of

the image data. Image segmentation can be defined as the process of partitioning an image into disjoint but connected sets of pixels, referred to as objects and background. A detailed overview over segmentation methods can be found in [5]. In this work we concentrate on region growing techniques, which take the basic approach of classifying pixels on its position and the surrounding region. We obtain homogeneous regions from the image through a growth process, which starting from a preselected seed, progressively agglomerates points around it satisfying a specified homogeneity criterion. The growth process stops when no more points can be added to the region. The main advantage of this technique is that the regions obtained are certainly spatially connected and rather compact. As a threshold parameter to terminate the region growing algorithm, we choose an intensity threshold, which separates the objects from the background. To determine the threshold intensity we employed the triangle thresholding algorithm due to [10]. The reason for choosing this technique is that the image grey-level histogram is bimodal or nearly bimodal, whereby the object pixels produce a weak peak compared to the distinct main peak of the background. Additionally image segmentation can be enhanced by postprocessing with morphological filtering ([6]) to facilitate the feature detection. The most useful morphological operations are *opening* and *closing*, including tasks such as smoothing out object outlines, filling small holes, connecting disjoint objects, eliminating small bridges and branches.

3.2.2 Object Classification

The image objects having extracted still need to be classified. Since airborne dust particles usually have no regular geometric shape, for a first classification of PM_{10} particular shape features including object area, center of mass, perimeter and maximal diameter are computed. As a grey level feature we take into account the mean intensity of the objects.

Let P be an segmented object, consisting of the set of pixels $\{(x_i, y_i); i \in I\}$, where I denotes set of pixel indexes. The *mass* of an object P is defined as

$$mass := \sum_{i \in I} u(x_i, y_i) \ ,$$

whereby $u(x, y)$ is considered as the smoothed, fused image described in section 3.1. The *area* is measured in pixels and indicates the relative size of the object P. The *mean intensity* is defined as the ratio of the object mass and object area. The *object center* is given as

$$\begin{pmatrix} x_c \\ y_c \end{pmatrix} := \frac{1}{mass} \sum_{i \in I} u(x_i, y_i) \begin{pmatrix} x_i \\ y_i \end{pmatrix} .$$

The *maximal radius* of P, referred to as *thickness*, corresponds to the maximal euclidean distance of all object pixels to the object center, i.e.

$$\max_{i \in I} \sqrt{(x_i - x_c)^2 + (y_i - y_c)^2} \ .$$

All objects with a mean intensity in between a certain range, with a minimum size of pixels and a maximal thickness are detected according to a user defined threshold feature vector. The last step of our algorithm consists in counting the objects less than 10μm in diameter.

4 Results

For testing the performance of the proposed detection algorithm, microscope slides were scanned in z-direction, providing stacks of three greyscale images at a spatial resolution of 0.28 μm per pixel over a 220μm by 160μm field of view. The preliminary results of the detection of PM_{10} are shown in figure 1 and 2. The upper left images show respectively the preprocessed fused images, containing small as well as comparable bigger airborne dust particles and single pollen grains. The upper right images show the smoothing results of the anisotropic diffusion filtering. The lower left images represent the results of segmentation, whereby only the objects which where segmented are shown. From the 114 candidates found for the first sample image, 25 are detected as airborne particles with maximal diameter less than 10μm, marked in the lower right image. For the second sample 40 from 92 segmented particles are detected as PM_{10}. The detection of the particles is controlled by three parameters, namely the minimal size, the minimal intensity difference from the background and the maximal radius related to the *thickness*.

The quality of the PM_{10} monitoring carried out by human eye varies according to the experience of the person counting the particles. Instead the automated PM_{10} recognition provides a reproducible well defined quality and with it a faster availability of the data. Furthermore the algorithm detects a significant amount of particles which are not obviously visible to the naked eye.

5 Discussion and Conclusion

In this paper we have presented an algorithm developed for digital recording, detection and statistical processing of collected PM-data. In its current state the algorithm comprises data acquisition including the treatment of different foci, pre-filtering based on anisotropic diffusion, segmentation and intensity based classification.
Current results are promising but also indicate possible improvements of the algorithms.
Further developments of the algorithm will concentrate on separation of close-by objects, enhancement of classification process based on multiple object features to provide robustness and statistical treatment of detected PM including temporal trends.

Acknowledgments: The work of Sylvia Leimgruber was supported by the trans IT of the University of Innsbruck and by the Tiroler Wissenschaftsfonds grant, Project UNI-0404/213. Sylvia Leimgruber is grateful for the project-related Raiffeisen-Landesbank-Förderpreis 2004

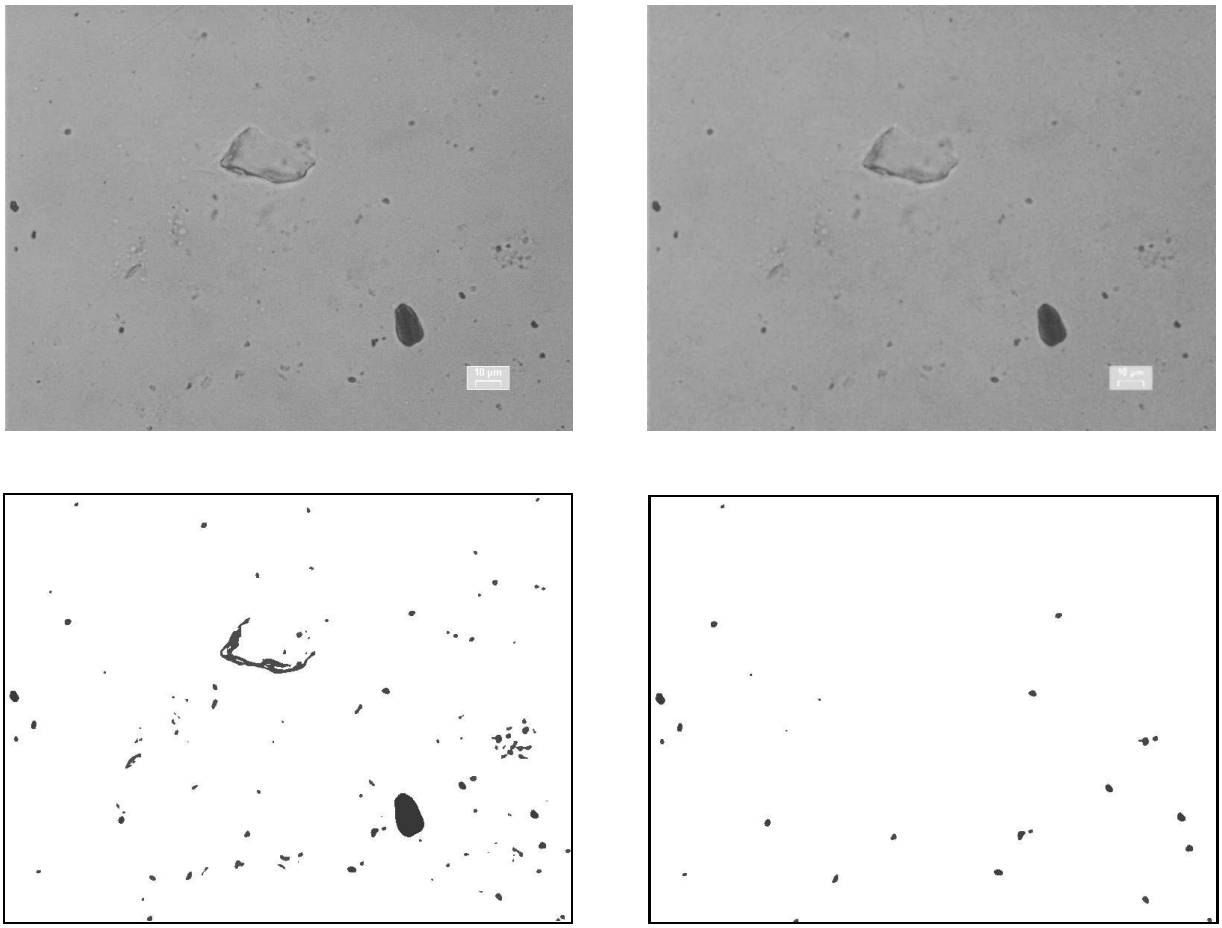

Figure 1: Top left: preprocessed image. Top right: image smoothed with anisotropic diffusion filtering. Bottom left: 114 segmented objects. Bottom right: 25 detected particles less than 10μm in diameter. Parameter settings for PM_{10} selection: minimal size 2, minimal intensity difference from background 0.15, thickness threshold 17.

of the University of Innsbruck. Furthermore we are indepted to Univ.-Prof. Dr. Bortenschlager for kindly providing the biological samples and for his support in scientific questions. We thank Werner Kofler from the Institute of Botany for making available the microscopic images.

References

[1] Bortenschlager, S. and Bortenschlager, I., 2003, Änderung des Pollenfluges durch Klimaerwärmung - Vergleichende Untersuchungen Innsbruck/Obergurgl über den Zeitraum 1980-2001, *Ber.nat.-med. Verein Innsbruck, 90:41-60.*

[2] Forster, B., Van de Ville, D., Berent, J., Sage, D., and Unser, M., 2004, Complex Wavelets for Extended Depth-of-Field: A New Method for the Fusion of Multichannel Microscopy Images, *Microscopy Research and Technique, 65:33-42.*

[3] Hinds, W.C., 1999, Aerosol Technology, Properties, behavior, and measurment of airborn particles, *John Wiley & Sons, New York.*

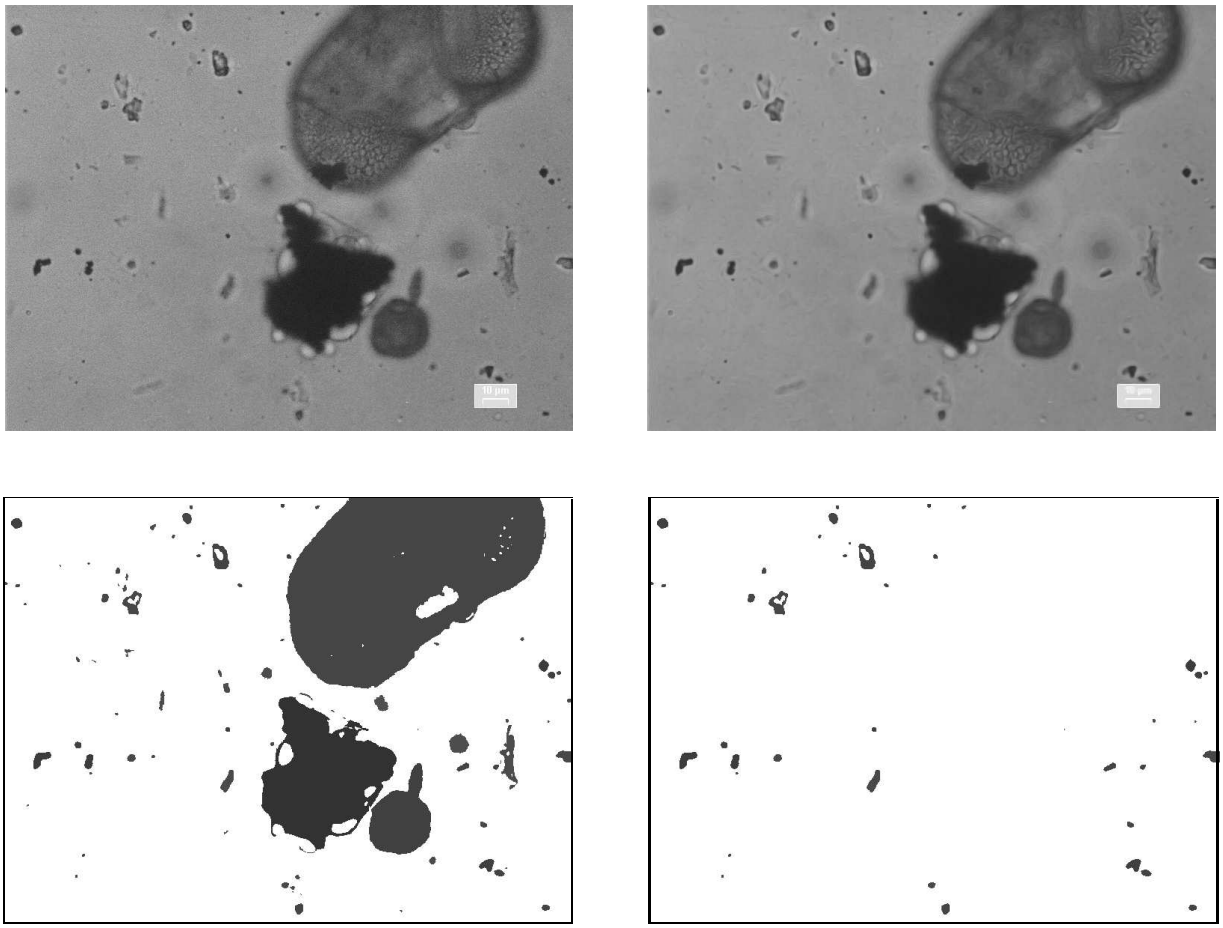

Figure 2: Top left: preprocessed image. Top right: image smoothed with anisotropic diffusion filtering. Bottom left: 92 segmented objects. Bottom right: 40 detected particles less than 10μm in diameter. Parameter settings for PM_{10} selection: minimal size 2, minimal intensity difference from background 0.15, thickness threshold 17.

[4] Perona, P. and Malik, J., 1990, Scale space and edge detection using anisotropic diffusion, *IEEE Trans.Pattern.Anal.Mach.Intell., 12:629-639.*

[5] Rosenfeld, A. and Kak, A.C., 1982, Digital picture processing, *vol.1-2, 2nd edition, Computer Science and Applied Mathematics.*

[6] Soille, P., 2004, Morphological Image Analysis: Principles and Applications, *Springer-Verlag, Berlin, New York.*

[7] Valdecasas, A.G., Marshall, D.,Becerra, J.M. and Terrero, J.J., 2001, On the extended depth of focus algorithms for bright field microscopy, *Micron 32:559-569.*

[8] Weickert, J., 1998, Anisotropic diffusion in image processing, *Teubner, Stuttgart.*

[9] Wichmann, H.E., Heinrich, J., Peters, A., 2002, Gesundheitliche Wirkungen von Feinstaub, *ecomed-Verlag, Landsberg.*

[10] Zack, G.W., Rogers, W.E. and Latt, S.A., 1977, Automatic measurement of sister chromatid exchange frequency, *J.Histochem.Cytochem., vol.25, no.7, pp.741-753.*

[11] `http://www.burkard.co.uk`